# Long-range tracking of thunderstorms using sferic measurements

T. G. Wood and U. S. Inan

STAR Laboratory, Stanford University, Stanford, California, USA

Received 16 December 2001; revised 16 May 2002; accepted 12 June 2002; published 5 November 2002.

[1] Each lightning stroke launches an electromagnetic pulse, known as a radio atmospheric or sferic that propagates in the waveguide between the Earth and the ionosphere. Sferics, with most of their energy contained in the frequency band from 3 Hz to 30 kHz, can propagate with low loss to distances of tens of megameters. Using very low frequency (VLF) magnetic field measurements at Palmer Station, Antarctica, the azimuths of sferics originating in North America (~10,000 km range) are found to be measurable to less than 1 degree accuracy. Analysis of the arrival azimuths at Palmer Station allows the assessment of lightning flash rates of storms occurring in diverse regions of the globe including North America and Africa. Arrival azimuths are compared with flash level data from the National Lightning Detection Network (NLDN) and 83.6% of the sferics that could be matched to NLDN flashes were within 2 degrees of the predicted azimuths for those flashes. Results are also compared with data from the satellite-based Optical Transient Detector (OTD), and the arrival azimuths of sferics detected at Palmer Station are consistent with the location of lightning occurring elsewhere around the world. The relative distribution of and the relationship between ground flashes and cloud flashes are discussed for a specific localized thunderstorm. Evidence that sferics generated by intracloud discharges were detected at Palmer Station is also presented. *INDEX TERMS:* 0624 Electromagnetics: Guided waves; 0689 Electromagnetics: Wave propagation (4275); 3324 Meteorology and Atmospheric Dynamics: Lightning; 3360 Meteorology and Atmospheric Dynamics: Remote sensing; *KEYWORDS:* lightning detection, storm dynamics, magnetic direction finding

**Citation:** Wood, T. G., and U. S. Inan, Long-range tracking of thunderstorms using sferic measurements, *J. Geophys. Res.*, *107*(D21), 4553, doi:10.1029/2001JD002008, 2002.

## 1. Introduction

[2] Lightning and thunderstorms have been observed for hundreds of years with steadily increasing sophistication as available monitoring technology has advanced. In the early twentieth century, thunderstorm observations were coarsely recorded by noting whether or not lightning had been seen or thunder heard on a particular day [*Brooks*, 1925]. Today, ground-based networks such as the National Lightning Detection Network (NLDN) in North America [*Cummins et al.*, 1998] and space-based instruments such as the Optical Transient Detector (OTD) [*Christian et al.*, 1996] and the Lightning Imaging Sensor (LIS) [*Christian et al.*, 1999b] are used to accurately determine the time and location of individual lightning strokes and flashes.

[3] The first attempt to study lightning and thunderstorms on a global scale was made by Brooks in 1925 [*Brooks*, 1925]. Using sparse, often unreliable meteorological records and a lot of educated guessing, Brooks estimated the global lightning flash rate to be ~100 lightning flashes per second. Over 50 years later, based on continued measurements over that period, Orville derived a remarkably similar value [*Orville and Spencer*, 1979]. More recent estimates based on satellite observations indicate the global flash rate may be somewhat lower at ~40 lightning flashes per second [*Christian et al.*, 1999a]. Although a single value is often quoted as the global flash rate, the lightning flash rate for any particular area varies significantly over the course of a day and from season to season. Also, some lightning "hot spots" located around the globe are naturally more active than other locations.

[4] Modern lightning detection systems vary in their detection capabilities and coverage area. The NLDN provides high spatial and time resolution for cloud-to-ground (ground) flashes with continuous coverage in North America but discriminates against intracloud activity [*Cummins et al.*, 1998]. The NLDN also has an overall detection efficiency of about 85% for cloud-to-ground lightning [*Cummins et. al.*, 1998]. Space-borne instruments such at the OTD and LIS aboard low Earth orbiting satellites provide near global coverage and record both ground flashes and intracloud and cloud-to-cloud (cloud) flashes with a 50% detection efficiency, but cannot distinguish between the two [*Christian et al.*, 1996, 1999b]. However, with these low Earth orbit satellite systems, any particular area of the globe only falls within their fields of view for a limited amount of time each day. Also, it takes about 50 days for the OTD to pass over the same point on Earth at the same time of day [*Christian et al.*, 1996]. It is thus highly desirable to utilize ground-based measurements to track global lightning activity on a continuous basis. The results presented in this paper


0148-0227/02/2001JD002008$09.00

indicate that long range sferic measurements may be useful in this endeavor.

## 2. Sferic Propagation

[5] Each lightning stroke radiates an electromagnetic pulse known as a radio atmospheric or sferic. The energy in these pulses ranges from a few hertz [*Fraser-Smith*, 1993] up to tens of megahertz [*Weidman and Krider*, 1986]. However, due to the timescales and spatial extents of lightning discharges, the majority of this energy is contained in the extremely low frequency (ELF) and very low frequency (VLF) bands ranging from 3 Hz to 30 kHz [*Uman*, 1987, p. 118]. At ELF and VLF frequencies, sferics propagate with low loss, typically 2–3 dB/1000 km [*Davies*, 1990, p. 367], through the waveguide formed by the Earth and the ionosphere and can therefore be detected at great distances (>10,000 km) from their source locations [*Davies*, 1990, p. 367]. The Earth-ionosphere waveguide is bounded by the conducting ground on one side and by the lower ionosphere on the other with a separation distance of ~70 km in the daytime and ~85 km at night [*Thomson*, 1993]. Furthermore, the actual attenuation rate for the VLF/ELF waves varies depending on the propagation conditions, with the lowest attenuation occurring along a sea path at nighttime [*Davies*, 1965, p. 426].

[6] Lightning flashes can be roughly classified into two groups; cloud flashes, those that do not terminate at the Earth's surface, and ground flashes, those with at least a partial discharge to the Earth's surface [*Prentice and Mackerras*, 1977]. Historically, cloud flashes are the most numerous type of lightning but also the hardest to definitively identify [*Prentice and Mackerras*, 1977]. For long-range detection of sferics, it is important to consider the propagation characteristics of modes generated by these two types of lightning. Vertical discharges, indicative of ground flashes, exhibit a maximum in their radiation pattern at low elevation angles [*Jordan and Balmain*, 1968, pp. 641–644]. Considering propagating modes in the Earth-ionosphere waveguide as a superposition of uniform plane waves, wave energy launched at such low elevation angles preferentially excites lower order waveguide modes [*Inan and Inan*, 1999, pp. 269–271], which in turn have lower attenuation rates [*Wait*, 1957]. Cloud flashes, while also often occurring primarily as a vertical discharge, frequently consist of a horizontal discharge as well [*Krehbiel*, 1986]. In contrast to vertical discharges, horizontal discharges exhibit a null in their radiation patterns at low elevation angles [*Jordan and Balmain*, 1968, pp. 641–644] and thus preferentially excite higher order waveguide modes with higher rates of attenuation. However, both the upper and lower boundaries of the earth-ionosphere waveguide are not uniform and these higher order modes can couple to lower order modes at discontinuities at land-sea or day-night boundaries [*Wait*, 1968] allowing sferics generated by horizontal cloud flashes to be detectable at great distances.

## 3. Sferic Detection and Direction Finding

[7] As discussed above, sferics can propagate to great distances Earth-ionosphere waveguide and are detectable using VLF receivers at remote locations. One such receiver is located at Palmer Station (Palmer) on Anvers Island off the coast of the Antarctic peninsula. The Stanford-built ELF/VLF receiver at Palmer utilizes two crossed magnetic loop antennas and signal conditioning electronics that provide a flat frequency response between ~100 Hz and ~22 kHz [*Reising*, 1998]. The antennas are positioned orthogonal to each other and are designated North/South (N/S) and East/West (E/W). Historically, the N/S antenna at Palmer was oriented with its plane parallel to a magnetic meridian so that it was aligned with geomagnetic coordinates. However, for the purposes of direction finding, a simple rotation is performed in post processing to convert to geographic coordinates. The broadband magnetic field signals from the two antennas are sampled using a PCM encoder with a cutoff frequency of about 20 kHz. The resulting digital signals are recorded on magnetic tape along with an IRIG-B timing signal with 1-ms absolute time resolution. More recent data (not used here) is sampled at 100 kHz and has 10-microsecond absolute time resolution.

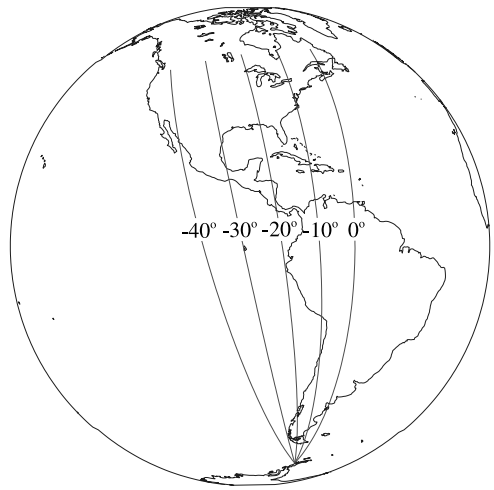


**Figure 1.** The lines represent the great circle paths from North America to Palmer Station, Antarctica. The values −40° to 0° indicate the arrival azimuth for these paths at Palmer Station.

[8] Like any radio signal, the recorded VLF signals are distorted by ambient noise. Some of the largest noise sources in the VLF range are power lines that radiate 60 Hz as well as harmonics of 60 Hz. One of the advantages of making observations in a remote location such as Palmer Station is that it is far away from population centers and thus from power lines as well. Other sources of interference include natural signals such as whistlers and chorus [*Helliwell*, 1965, pp. 83 and 207] and manmade signals such as the Omega and Alpha navigation transmitters in the 10–14 kHz range. (The Omega transmitters have since been decommissioned. However, they are considered here since the data was acquired before 1998.) In this kind of ambient noise environment a sophisticated algorithm must be used to detect and analyze the impulsive, broadband sferic waveforms.

[9] The first step in isolating a sferic waveform is to filter the broadband signal around the frequency band of interest. In this study the band from 5.5 to 9.5 kHz was used. This frequency range contains a large amount of energy from sferics and little interference from power lines, whistlers, and

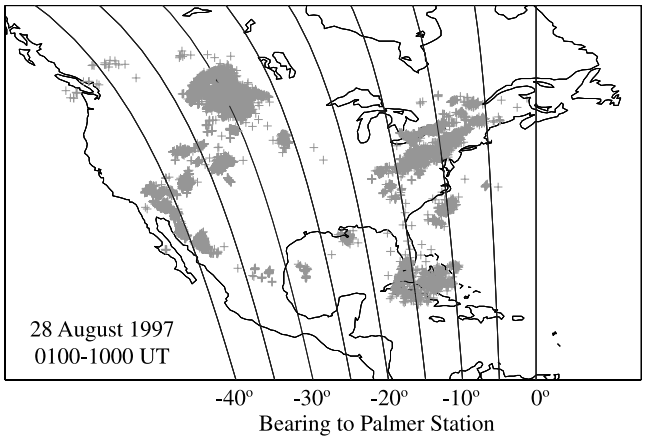


**Figure 2.** Each crosshair represents the location of an NLDN recorded cloud-to-ground lightning flash. The lines represent the great circle paths to Palmer Station.

Omega transmitters. Also, zero phase filters are used to preserve the phase relationships between the frequencies. Once the signals are bandpass filtered they are combined to obtain the absolute field strength of the signal. Since sferics are broadband impulsive signals, the 22-kHz cutoff frequency of the VLF receiver necessarily introduces "ringing" into the sferic waveform. In an attempt to create a single maximum for each sferic, the absolute magnetic field signal is low-pass filtered. Since a single peak for each sferic is not always obtained, an additional constraint is imposed on the detection process such that the next sferic can not be detected within 2 ms of a previously detected one. Maxima in the filtered absolute magnetic field signal that exceed a specified threshold are considered possible sferics, and their times are recorded at the maximum of each peak. To verify that the peak is in fact a sferic the band pass filtered signals for that peak are then subjected to a phase coherence test. This test requires that the signals from the two channels be either in phase or 180 degrees out of phase with each other to a specified tolerance, typically about 30 degrees.

[10] Once a sferic is detected and its arrival time is determined, its arrival azimuth is calculated using magnetic direction finding in the Fourier domain. This technique uses a weighted average of the sferic energy over a certain frequency range and the phase relationship between the two signals to determine the arrival azimuth ambiguous by 180 degrees. The accuracy of this method was verified using the Omega navigation transmitters [*Burgess*, 1993]. Results become difficult to interpret in the presence of simultaneously arriving signals such as when two sferics arrive from different directions [*Burgess*, 1993].

[11] With the sferic azimuths so determined, the performance of the direction finding algorithm is evaluated using independent data on the source lightning locations. Figure 1 shows selected great circle bearings from North America to Palmer Station, located ~12,000 km away. Some of these paths, such as the $-40°$ bearing, are predominantly over ocean, while others, such as the $-10°$ bearing, cross multiple land/sea boundaries. These differences are important because they may cause the signal to deviate from the great circle paths and may lead to errors in locating the causative lightning stroke [*Wait*, 1968]. Figure 2 shows the locations of lightning flashes detected by the NLDN from 0100–1000 UT on August 28, 1997. These flash locations are known with an accuracy of better than 0.5 km of their actual locations [*Cummins et al.*, 1998], equivalent to an accuracy of less than 0.003 degrees at Palmer Station, well beyond the resolution of this long-range sferic direction finding system. Therefore, for the purposes of this study, the NLDN flash locations can be considered to be exact.

[12] For the day shown in Figure 2, major storm centers are located off the coast of Florida, across the northeast, in the northern Midwest, and along the Gulf of California. Smaller storms are also present, such as the one off the coast of Louisiana along a bearing of about $-22°$. The performance of the direction finding algorithm is evaluated with data from Palmer Station by means of a one-to-one association between sferics detected at Palmer Station and their causative cloud-to-ground lightning flashes as detected by the NLDN. Individual sferics are created by the return strokes of a lightning flash [*Uman*, 1987, pp. 110–120]. However, due to the great distance to Palmer Station from North America, it is assumed that most of the sferics originating in North America and detected at Palmer Station were generated by the first return strokes of lightning flashes (the radiated power of first return strokes typically exceeds that of subsequent strokes by a factor of ~2 to 5 [*Uman*, 1987, pp. 122–123; *Krider and Guo*, 1983]), depending also on the thresholding imposed during analysis. Therefore, since flash level NLDN data is being used to match sferics to NLDN data, the phrase "NLDN flash" henceforth implies a comparison to the first return stroke of the lightning flash detected by the NLDN.

[13] By assuming propagation along great circle bearings the expected arrival azimuth at Palmer Station of a sferic generated by a North American lightning flash can be calculated. Also, for low-order modes, propagation through the waveguide occurs at near the speed of light [*Budden*, 1961, p. 69] and therefore, the expected arrival time of a

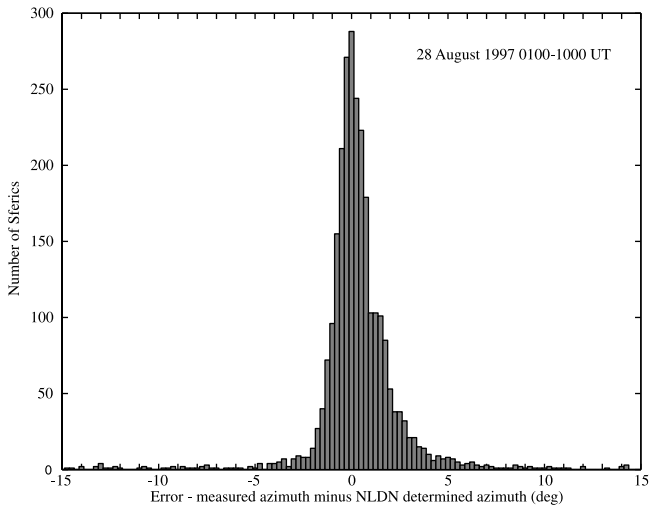


**Figure 3.** Histogram of the errors between arrival azimuths calculated from NLDN data and azimuths obtained from using VLF magnetic direction finding at Palmer Station, Antarctica. Over a 9-hour period, 2771 sferic azimuths were matched to NLDN flashes with 63.0% accurate to within 1° and 83.6% accurate to within 2°.

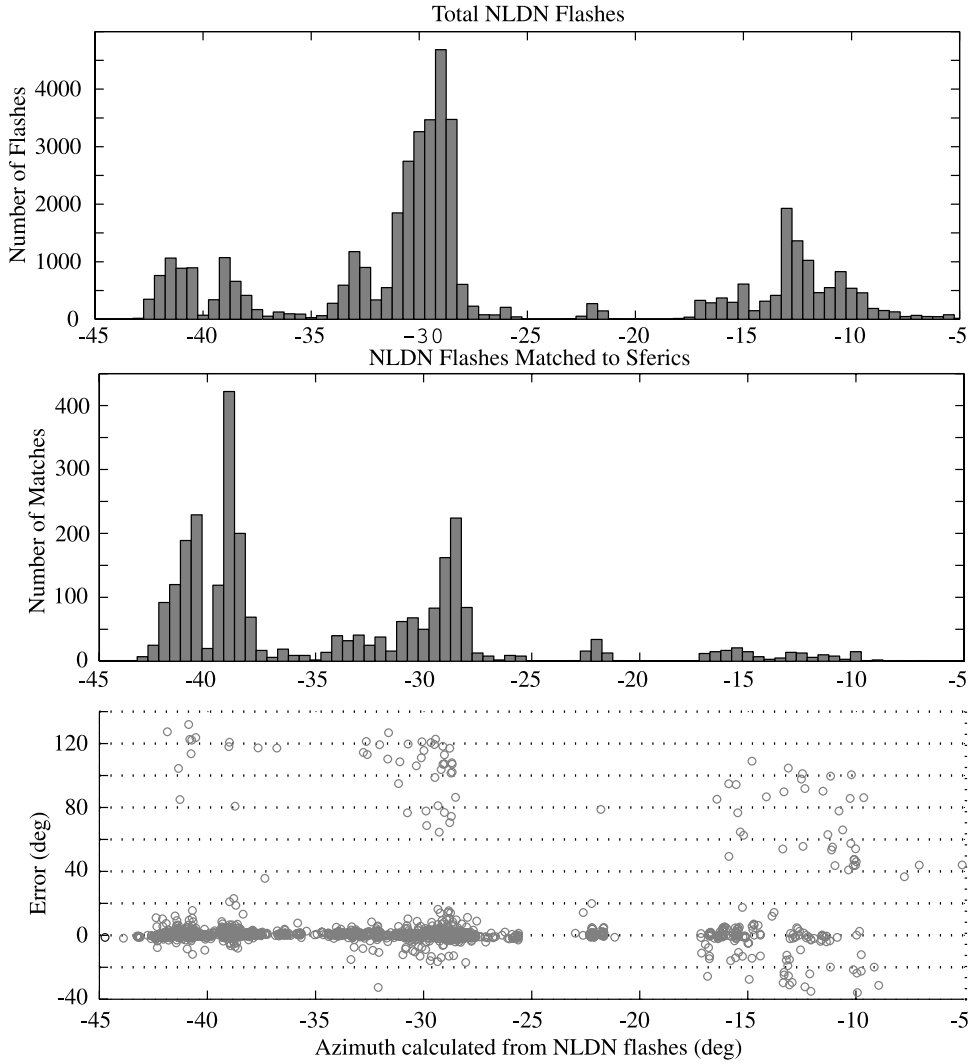


**Figure 4.** A comparison between the arrival azimuth calculated from NLDN data and azimuths measured at Palmer Station relative to the arrival azimuth. In the bottom panel, notice that many of the sferics with large errors are clustered together indicated that they were probably mismatched to NLDN flashes and that the causative lightning was probably located outside of North America.

sferic can be calculated with ~1 ms accuracy. For lightning flashes in North America, propagation to Palmer Station takes 30–40 ms. Since the arrival time of a sferic detected at Palmer Station is measured with 1-ms resolution, all sferics arriving within 1.5 ms of the expected arrival times of sferics radiated by NLDN flashes are considered to match to those NLDN flashes. For sferics matched to NLDN flashes, the arrival azimuth error is the difference between the azimuth predicted using NLDN data and the azimuth calculated at Palmer Station. In practice, it is possible for another sferic from another storm to arrive simultaneously from a different direction, resulting in a large apparent error between NLDN location and arrival azimuth at Palmer Station.

[14] During the 9-hour period used in this study, 2771 sferics detected at Palmer Station were matched to NLDN flashes. Of these sferics, 60.5% were accurate to within 1 degree while 80.3% were accurate to within 2 degrees. Figure 3 shows a histogram of errors between the azimuths calculated at Palmer Station and the azimuths predicted from NLDN flashes for those sferics with an error of less than 15 degrees. For sferics with an azimuth error of less than 15 degrees, 63.0% are accurate to within 1 degree and 83.6% are accurate to within 2 degrees. The accuracy of sferics with less than 15 degrees of error is considered to be the actual performance because it is likely that sferics with very large errors were erroneously mismatched to NLDN flashes and may actually have originated from different locations.

[15] The first panel of Figure 4 shows the predicted azimuths for all NLDN flashes detected between 0100–1000 UT while the second panel shows only the azimuths for the sferics detected at Palmer Station that were matched to NLDN flashes. Notice that a higher percentage of the NLDN flashes with predicted arrival azimuths near $-40^\circ$ are matched to sferics than NLDN flashes with predicted azimuths near $-30^\circ$. This result is reasonable because Figure 2 shows that the lightning flashes along the $-30^\circ$ bearing are at a greater distance from Palmer Station than those lightning flashes along the $-40^\circ$ bearing. Therefore, the intensity of more of the sferics originating along the $-30^\circ$ bearing as opposed to those originating along the $-40^\circ$ bearing should

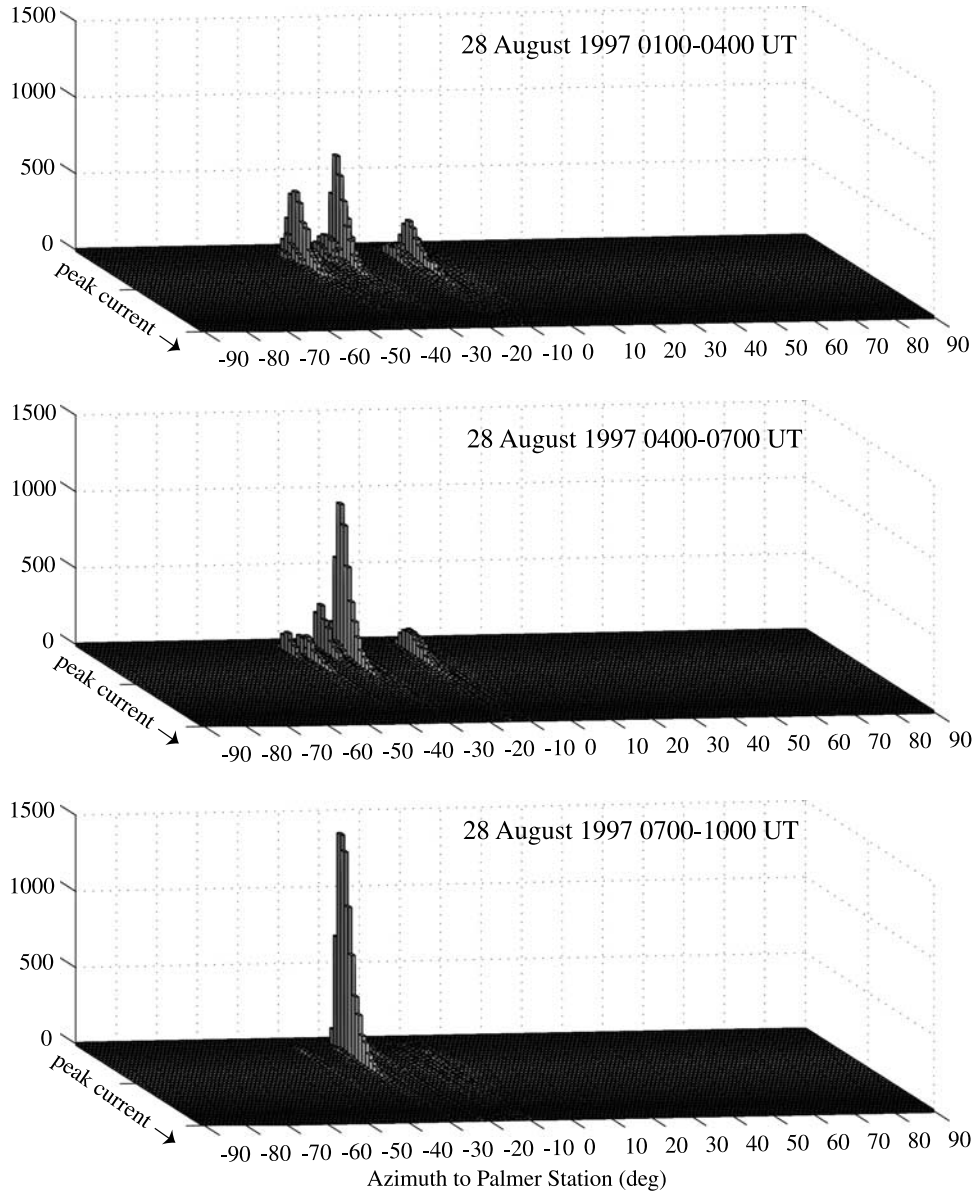


**Figure 5.** Histograms of arrival azimuths calculated from NLDN data for three consecutive 3-hour periods.

have attenuated below the detection threshold by the time they reach Palmer Station. An even smaller percentage of the NLDN flashes detected along the east coast of the United States were matched to sferics, possibly because the propagation path from the east coast crosses the South American continent. A propagation path primarily over land has a higher attenuation rate than a path over the sea due to the lower conductivity of the ground versus seawater [*Wait*, 1957]. The third panel of Figure 4 shows the errors for individual sferics versus their predicted arrival azimuths. Note that sferics with very large errors in azimuth appear to be clustered together with other sferics that have similarly large errors in azimuth. For example, a large number of sferic azimuths were calculated with 100–120° of error, suggesting that these sferics were mismatched to NLDN flashes and that they actually originated from a storm along a different azimuth. It is important to note that during the period of this study (0100–1000 UT) the entire path from North America to Palmer Station falls under the nighttime ionosphere. VLF attenuation rates are generally higher under daytime ionospheric conditions so that a fewer number of sferics would be detectable at Palmer Station. In addition, propagation paths crossing the day/night boundary may lead to additional error.

## 4. Thunderstorm Detection

[16] With the location accuracy for individual lightning strokes established, some characteristics of thunderstorms can be examined. Figure 5 shows histograms of projected azimuths for NDLN flashes for three consecutive 3-hour periods. Notice that the number of flashes detected with a projected azimuth of approximately −30° increases threefold from the first period to the third period. Also, the number of flashes with projected azimuths near −12° is greatly reduced

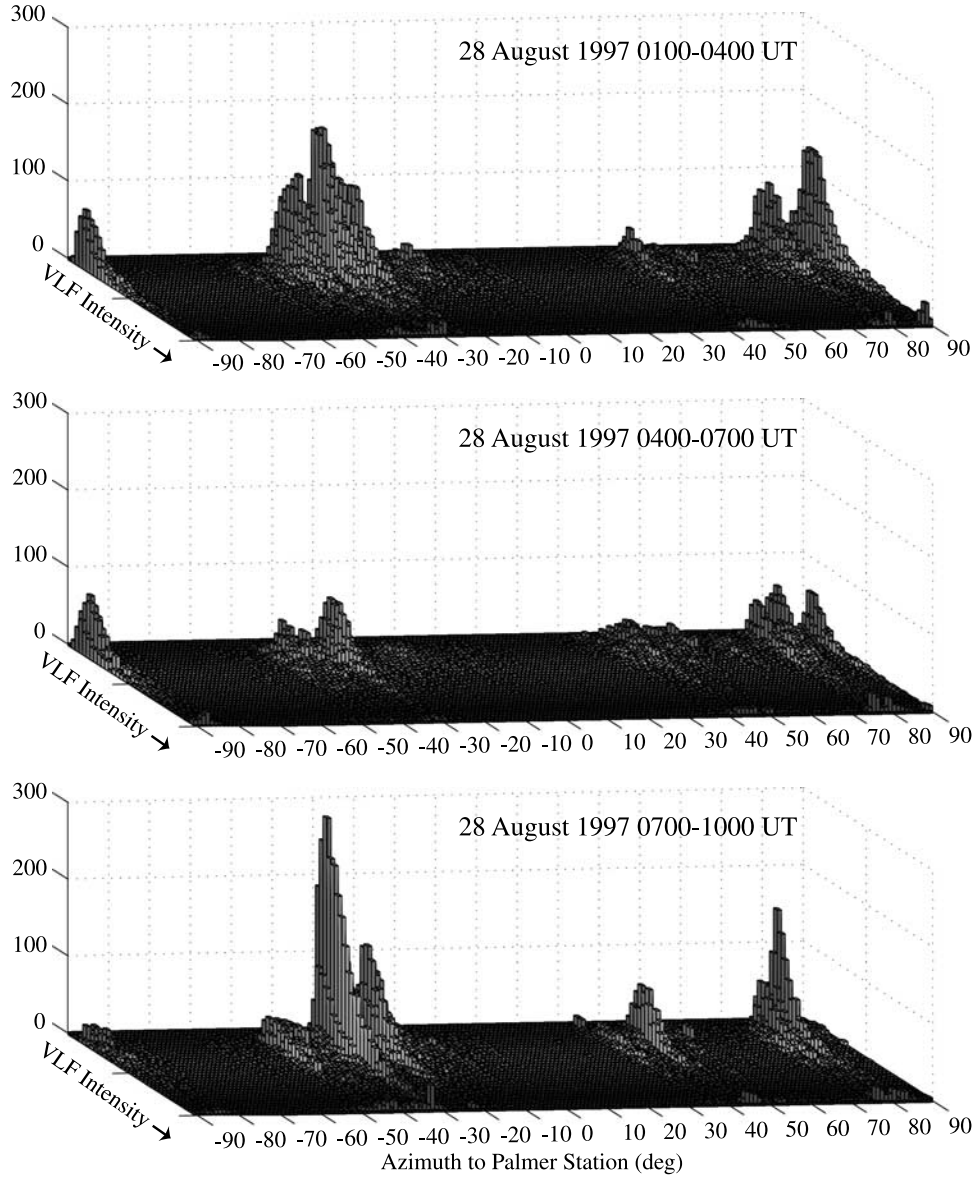


**Figure 6.** Histograms of arrival azimuths measured from sferics detected at Palmer Station, Antarctica for three consecutive 3-hour periods.

from the first period to the last period. Figure 6 shows histograms of the arrival azimuths for sferics detected at Palmer Station for the same 3-hour periods. Note that the number of sferics detected with an azimuth near $-30^\circ$ during the third period is nearly twice the number detected during the first period. Also, a significant number of sferics were detected with an azimuth near $-12^\circ$ during the first period while very few were present during the third period. While variations of the peaks from one 3-hour period to the next do not correspond precisely between Figure 5 and Figure 6, the overall behavior is quite similar. Also of interest in Figure 6 are the regions in azimuth where few if any sferics are detected. Since it has already been established that the sferics detected at Palmer Station originate in areas where there is lightning activity present, a lack of sferics detected along particular azimuth regions must indicate areas where there is little or no lightning activity present.

[17] In relatively rare cases, two or more storms may be simultaneously active and located along the same azimuth bearing from Palmer Station, making it difficult to determine the storms in which particular sferics originate. This limitation could be overcome by triangulating lightning locations using sferic data from multiple, suitably spaced receivers. Also note that there are additional peaks in Figure 6 that do not match to peaks in Figure 5. Since the receiver at Palmer Station can detect sferics arriving from all directions, these additional regions of high sferic occurrence indicate the presence of storms in other parts of the world outside of North America.

[18] The first panel of Figure 7 shows the locations of flashes detected by the OTD from 0100–1000 UT along with several great circle paths to Palmer. The OTD coverage is limited in that it can see most points on Earth for only about 14 hours over the course of a year [*Christian*, 1999a].

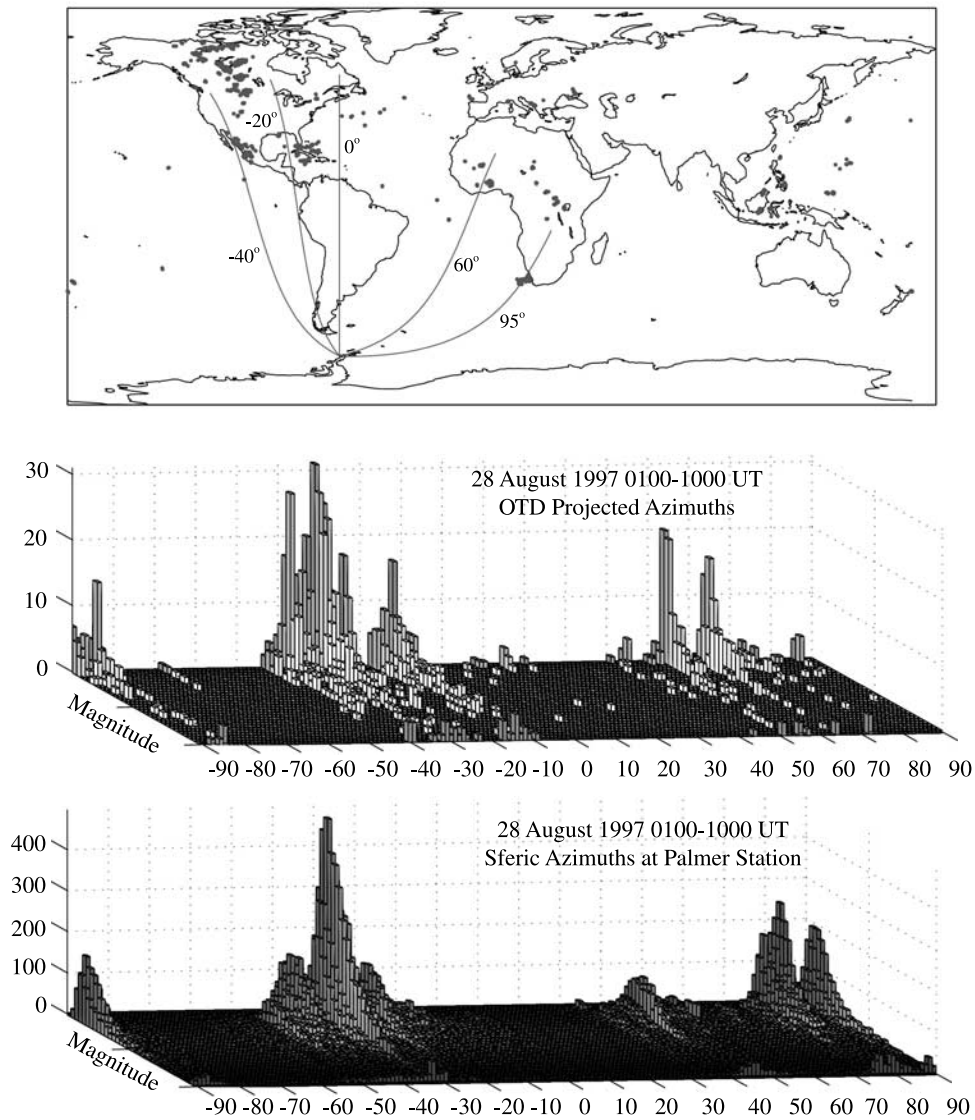


**Figure 7.** The top panel shows locations of lightning detected by the OTD over a 9-hour period from 0100–1000 UT. The middle panel shows the arrival azimuths calculated from the OTD detected lightning locations. The bottom panel shows the arrival azimuths measured for sferics at Palmer Station. Notice that the general pattern of peaks present in the OTD data is also present in the Palmer Station data.

The second panel shows a histogram of azimuths projected from OTD flash locations. The projected azimuths that cross the Antarctic continent were not counted because propagation over ice causes high attenuation [*Rogers and Peden*, 1975] and, in practice, it is unlikely that sferics propagating over Antarctica would be detectable at Palmer. The third panel of Figure 7 shows the arrival azimuths of sferics detected at Palmer Station from 0100–1000 UT. Both the second and third panels show activity in the 90° to 95° range (recorded at Palmer as −90° to −85° due to the 180° ambiguity). This correlation strongly suggests that the sferics detected with azimuths in this range originated from the storm located off the coast of South Africa. At the same time, we note that the other peaks in the histograms do not match up as well to storms seen by OTD. However, it should be noted that the receiver at Palmer is capable of detecting sferics from all directions at all times. Therefore, the other peaks in the third panel (50°, 80°, 85°) may identify storms, such as those in central Africa, that became more active while out of the field of view of the OTD.

## 5. Thunderstorm Monitoring

[19] Since the detection of sferics over an extended period of time allows thunderstorms to be monitored, it is now possible, in some cases, to track the flash rate of storms. Figure 2 shows a small, localized storm located off the coast of Louisiana along a great circle bearing of −22°. This storm is interesting in that no other North American storm is located along this azimuth during the 0100–1000 UT time period. The dashed curve in Figure 8 represents the number of sferics detected with and azimuth between −21° and

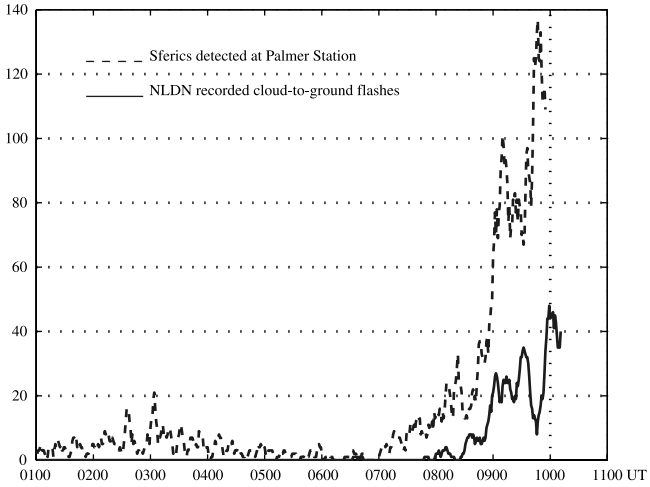


**Figure 8.** A flash rate comparison between sferics detected at Palmer Station with an azimuth between −21° and −23° and NLDN CG flashes with calculated azimuths between −21° and −23°. The two curves are correlated with a linear correlation coefficient of 0.88.

−23°. The third panel of Figure 4 shows that many of these sferics were correctly matched to NLDN recorded flash times. The dashed curve in Figure 8 shows the sum of all sferics detected over the previous five minutes with the calculation made each minute. The solid curve represents the projected azimuths of all the NLDN detected cloud-to-ground flashes in the same azimuth range, −21° to −23°, not just those matched to sferics detected at Palmer Station. These two curves are correlated with a linear correlation coefficient of 0.88 suggesting that the sferic detection rate at Palmer Station is proportional to the NLDN cloud-to-ground flash rate for this storm. Also, the number of sferics detected at Palmer Station is approximately 3 times the number of cloud-to-ground flashes recorded by NLDN. This difference could, in principle, be due to sferics produced by the subsequent return strokes of the NLDN detected lightning flashes. However, the geometric mean interval between return strokes is ∼58 ms [*Thomson*, 1980] whereas the geometric mean inter-arrival period between the sferics detected in this example is about ∼80 ms for sferics arriving within 300 ms of each other. Also, many of the additional sferics have magnitudes that are just as large, if not larger, than the magnitudes of sferics matched to NLDN flash times (first return strokes). Since the first return stroke typically has a peak current that is twice that of subsequent strokes [*Uman*, 1987, pp. 122–123], the additional sferics would not have such large magnitudes if they were generated by subsequent return strokes.

[20] Another possibility is that the additional sferics observed at Palmer may be due to intracloud flashes produced by the same storm, which are not detected (by design) by the NLDN. In this connection, it is intriguing to note the apparent ∼15 minute delay between the dashed and solid curves in Figure 8. In fact, if the sferic detection rate curve is delayed by 15 minutes min, the linear correlation coefficient between the two curves increases to 0.94. *Krehbiel* [1986] observed a delay of 5–10 min between the first intracloud flashes and the first ground flashes in some storms. Furthermore, a formula developed by *Prentice and Mackerras* [1977] provides an empirical relationship for the expected ratio, Z, of the number of cloud flashes to the number of ground flashes in a storm as a function of latitude, λ [*Prentice and Mackerras*, 1977].

$$Z(\lambda) = 4.16 + 2.16 \cos 3\lambda.$$

For the storm of interest located at approximately λ = 29°, north latitude, the expected ratio is 4.2. Considering that the strengths of sferics arriving at Palmer Station must be above a specified threshold to be detected, this value is consistent with the 3 to 1 ratio between sferics detected at Palmer Station and NLDN detected ground flashes. Thus, it is possible that many of the sferics detected at Palmer Station were generated by intracloud flash strokes and that periods of increased intracloud lightning activity are followed by a delayed but proportional increase in cloud-to-ground lightning activity in this particular storm.

[21] Further analysis of the sferics arriving in the −21° to −23° azimuth range reveals another interesting result. The ratio of the VLF peak intensity (the intensity of the band limited signal between 5.5 and 9.5 kHz) to the ELF peak intensity (the intensity of the signal below 1.5 kHz) is 14 percent higher for the sferics matched to NLDN flashes than the ratio found in the other sferics detected along this azimuth range. The cutoff frequency of the first mode of the Earth-ionosphere waveguide occurs at ∼1.7 kHz [*Porrat et al.*, 2001]. Therefore propagation of the energy below 1.5 kHz in the sferic waveforms must occur as a quasi-TEM mode wave since all the other modes will be evanescent at these frequencies. Figure 9 shows sketches of the radiation patterns for a vertical dipole at the surface of the earth, a horizontal dipole elevated above the earth and a vertical dipole elevated above the earth [*Jordan and Balmain*, 1968,

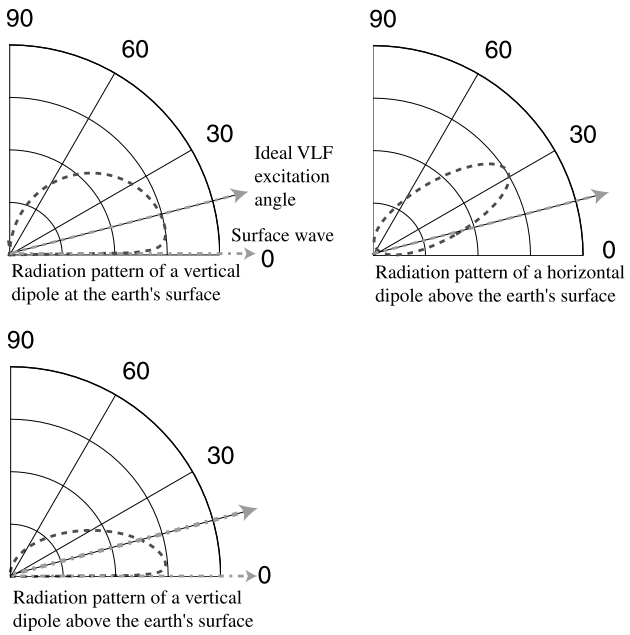


**Figure 9.** Radiation patterns for three different lightning source polarizations: a vertical discharge to the Earth's surface, a horizontal discharge above the Earth's surface, and a vertical discharge above the Earth's surface.

pp. 641–644]. The pattern for the horizontal dipole has a null for low elevation angles. Since the quasi-TEM ELF waves propagate with low elevation angles, the ratio of the VLF intensity to the ELF intensity for a horizontal discharge should be relatively higher than the corresponding ratio for a vertical discharge to ground, which exhibits a maximum in its radiation pattern at low elevation angles. A higher VLF to ELF ratio is inconsistent with the observations, suggesting that the additional sferics detected at Palmer Station may not have been generated by horizontal intracloud discharges.

[22] The radiation pattern for a vertical dipole above the Earth's surface has a maximum at low elevation angles similar to the maximum in the radiation pattern for a vertical dipole at the Earth's surface. However, as the elevation angle increases, the gain for the vertical dipole above the Earth drops off faster than the gain for the vertical dipole at the Earth's surface. Moreover, at the optimal excitation angles for the VLF range of interest (5.5–9.5 kHz) the gain for the vertical dipole above the earth is relatively less than the gain for vertical dipole at the earth's surface. Therefore, a vertical discharge above the earth's surface should have a smaller VLF/ELF ratio when compared to the VLF/ELF ratio for a vertical discharge to the Earth's surface. Since the ratio of VLF peak intensity to ELF peak intensity is higher for sferics matched to NLDN flashes than for the other sferics detected at Palmer Station, it is suggested that the additional sferics detected at Palmer Station were generated by intracloud lightning with a substantial vertical component.

[23] It is conceivable that there were other storms along the $-22^\circ$ azimuth out of the range of the NLDN (e.g., in South America) that could account for the larger number of sferics detected at Palmer Station. However OTD data does not contain any flashes along this path, or, for that matter, in South America during this time period. Furthermore, such a circumstance is unlikely in light of the high correlation between the sferic arrival rate and the NLDN flash rate for this storm. In particular, we note that there were virtually no sferics detected prior to the onset of the lightning activity around $\sim$0700 UT, so that if there were other storms they would have to coincidentally become active at or near the same time as the North American storm.

## 6. Summary

[24] We have demonstrated that the arrival azimuths for sferics generated by ground flashes in North America can be determined with a high degree of accuracy using measurements at Palmer Station, located over 10,000 km away from the source lightning flashes. We have also shown that sferics generated by lightning strokes over a wide range of the globe can also be detected at Palmer Station. Furthermore, the sferic arrival rate from a particular narrow azimuth range was correlated with the lightning flash rate for a particular storm indicating that lightning flash rates can be quantified with the long-range detection method discussed here. Also, it is believed that many of the sferics detected at Palmer Station were generated by intracloud lightning discharges.

[25] **Acknowledgments.** This research was supported by the National Science Foundation under grant OPP-9910565. T. Wood is partially supported by NASA under grant NGT 5-50227. NLDN data provided by the NASA Lightning Imaging Sensor (LIS) instrument team and the LIS data center via the Global Hydrology Resource Center (GHRC) located at the Global Hydrology and Climate Center (GHCC), Huntsville, Alabama through a license agreement with Global Atmospherics, Inc. (GAI). The data available from the GHRC are restricted to LIS science team collaborators and to NASA EOS and TRMM investigators. Special thanks goes to Ken Cummins of Global Atmospherics for information on the National Lightning Detection Network and to Jerry Yarbrough of Stanford University for his assistance with data analysis.

## References

Brooks, C. E. P., The distribution of thunderstorms over the globe, *Geophys. Mem.*, *3*(24), 147–164, 1925.

Budden, K. G., *The Wave-Guide Mode Theory of Wave Propagation*, Logos, London, 1961.

Burgess, W. C., Lightning-induced coupling of the radiation belts to geomagnetically conjugate ionospheric regions, Ph.D. thesis, Dep. of Elect. Eng., Stanford Univ., Stanford, Calif., March 1993.

Christian, H. J., K. T. Driscoll, S. J. Goodman, R. J. Blakeslee, D. A. Mach, and D. E. Buechler, The optical transient detector (OTD), paper presented at 10th International Conference on Atmospheric Electricity, NASA, Osaka, Japan, 1996.

Christian, H. J., et al., Global frequency and distribution of lightning as observed by the optical transient detector (OTD), paper presented at 11th International Conference on Atmospheric Electricity, NASA, Gunthersville, Ala., 1999a.

Christian, H. J., et al., The lightning imaging sensor, paper presented at 11th International Conference on Atmospheric Electricity, NASA, Gunthersville, Ala., 1999b.

Cummins, K. L., M. J. Murphy, E. A. Bardo, W. L. Hiscox, R. B. Pyle, and A. E. Pifer, A combined TOA/MDF technology upgrade of the U.S National Lightning Detection Network, *J. Geophys. Res.*, *103*, 9035–9044, 1998.

Davies, K., *Ionospheric Radio Propagation*, U.S. Dep. of Comm., Natl. Bur. of Stn., Gaithersburg, Md., 1965.

Davies, K., *Ionospheric Radio*, Peregrinus, London, 1990.

Fraser-Smith, A. C., ULF magnetic fields generated by electrical storms and their significance to geomagnetic pulsation generation, *Geophys. Res. Lett.*, *20*, 467–470, 1993.

Helliwell, R. A., *Whistlers and Related Ionospheric Phenomena*, Stanford Univ. Press, Stanford, Calif., 1965.

Inan, U. S., and A. S. Inan, *Electromagnetic Waves*, Prentice-Hall, Old Tappan, N. J., 1999.

Jordan, E. C., and K. G. Balmain, *Electromagnetic Waves and Radiating Systems*, 2nd ed., Prentice-Hall, Old Tappan, N. J., 1968.

Krehbiel, P. R., The Electrical structure of thunderstorms, in *The Earth's Electrical Environment*, pp. 90–113, Natl. Acad., Washington, D.C., 1986.

Krider, E. P., and C. Guo, The peak electromagnetic power radiated by lightning return strokes, *J. Geophys. Res.*, *88*, 8471–8474, 1983.

Orville, R. E., and D. W. Spencer, Global lightning flash frequency, *Mon. Weather Rev.*, *107*, 934–943, 1979.

Porrat, D., P. R. Bannister, and A. C. Fraser-Smith, Modal phenomena in the natural electromagnetic spectrum below 5 kHz, *Radio Sci.*, *36*, 499–506, 2001.

Prentice, S. A., and D. Mackerras, The ratio of cloud to cloud-to-ground lightning flashes in thunderstorms, *J. Appl. Meteorol.*, *16*, 545, 1977.

Reising, S. C., Remote sensing of the electrodynamic coupling between thunderstorm systems and the mesosphere/lower ionosphere, Ph.D. thesis, Stanford Univ., Stanford, Calif., 1998.

Rogers, J. C., and I. C. Peden, The VLF complex permittivity of deep Antarctic ice measured in situ, *Radio Sci.*, *10*, 763–771, 1975.

Thomson, E. M., The dependence of lightning return stroke characteristics on latitude, *J. Geophys. Res.*, *85*, 1050–1056, 1980.

Thomson, N. R., Experimental daytime VLF ionospheric parameters, *J. Atmos. Terr. Phys.*, *55*, 173, 1993.

Uman, M. A., *The Lightning Discharge, Int. Geophys. Ser.*, vol. 39, Academic, San Diego, Calif., 1987.

Wait, J. R., The attenuation vs. frequency characteristics of VLF waves, *Proc. IRE*, *45*, 768–771, 1957.

Wait, J. R., Mode conversion and refraction effects in the Earth-ionosphere waveguide for VLF radio waves, *J. Geophys. Res.*, *73*, 3537–3548, 1968.

Weidman, C. D., and E. P. Krider, The amplitude spectra of lightning radiation fields in the interval from 1 to 20 MHz, *Radio Sci.*, *21*, 964–970, 1986.

U. Inan and T. Wood, STAR Laboratory, Stanford University, Packard Building, Room 355, 350 Serra Mall, Stanford, CA 94305-9515, USA. (inan@nova.stanford.edu; twood@nova.stanford.edu)